Evidence for subwavelength imaging with positive refraction

Evidence for subwavelength imaging with positive refraction

Yun Gui Ma[1]**, Sahar Sahebdivan**[2]**, C K Ong**[3]**, Tomáš Tyc**[2,4]
and Ulf Leonhardt[2,5]

[1] Temasek Laboratories, National University of Singapore,
Singapore 119260, Singapore
[2] School of Physics and Astronomy, University of St Andrews, North Haugh,
St Andrews KY16 9SS, UK
[3] Centre for Superconducting and Magnetic Materials, Department of Physics,
National University of Singapore, Singapore 117542, Singapore
[4] Faculty of Science, Kotlarska 2 and Faculty of Informatics, Botanicka 68a,
Masaryk University, 61137 Brno, Czech Republic
E-mail: ulf@st-andrews.ac.uk

Abstract. The resolution of lenses is normally limited by the wave nature of light. Imaging with perfect resolution was believed to rely on negative refraction, but here we present experimental evidence for subwavelength imaging with positive refraction.

Ordinary lenses cannot resolve details finer than about half the wavelength of light [1]. Perfect lenses made of negatively refracting metamaterials were predicted [2] to image with unlimited resolution. In practice, however, passive negatively refracting materials have the disadvantage of being inherently dissipative [3]. Subwavelength details are dissipated away; only 'poor-man's perfect lenses' have worked [4]—they image over distances of merely a small fraction of the wavelength. Hyperlenses [5, 6] created magnified virtual images with a resolution limited by their geometric extensions. Time-reversed mirrors [7] made subwavelength images for electromagnetic microwaves, but with active devices that are difficult to implement for visible light.

Maxwell [8] showed that a lens with a particular spatial distribution of refractive index, 'Maxwell's fish eye', would, if analyzed by ray optics, give perfect resolution, i.e. a point source would give a point image. Ray optics ignores the wave nature of light and it

---

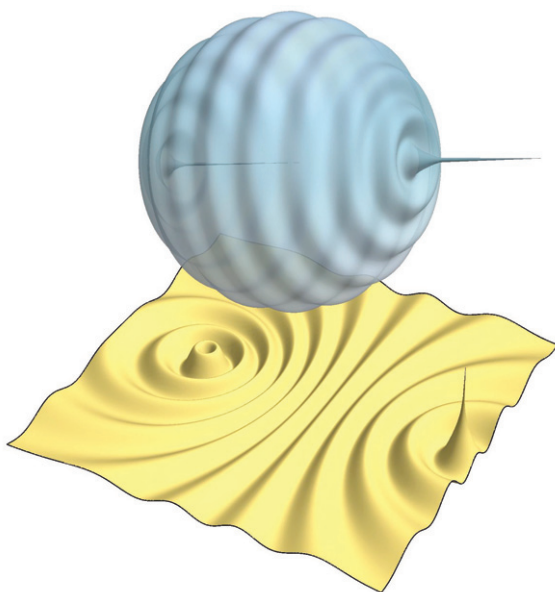[5] Author to whom any correspondence should be addressed.

Figure 1. Focusing in curved space. In Maxwell's fish eye, electromagnetic waves propagate in a plane in physical space (wave pattern below) as if they were confined to the surface of a sphere (above). A wave emitted from any point on the virtual sphere is focused at the antipodal point. In physical space, waves are as perfectly focused as in virtual space.

was assumed that in reality the resolution would again be about half the wavelength. We predicted that this is not so [9, 10]: Maxwell's fish eye should image waves with perfect resolution [11], which contradicted the accepted wisdom of subwavelength imaging [2] and created controversy [12]–[22]. Here, we present experimental evidence for subwavelength imaging over superwavelength distances in Maxwell's fish eye using microwaves. Like light, microwaves are electromagnetic waves, but with cm wavelenghts and GHz frequencies, which allow us to investigate the electromagnetic fields with a degree of detail currently impossible for visible light. Our microwave experiments establish the principle and encourage extensions to visible and shorter wavelengths [23, 24], and to other waves [11], such as sound.

Our experiments are inspired by the idea that optical materials change the geometry perceived by light [25], which can be represented by a spatial mapping [26]–[29]: light propagation in physical space corresponds to propagation in a transformed virtual space. For example, a negatively refracting perfect lens folds space [30]: in virtual space, a plane of physical space appears like a folded sheet of paper [25]. The electromagnetic fields in the folded regions are identical; they are 'carbon copies' of each other, which explains in a geometrical picture why negative refraction makes a perfect lens. In this case, the underlying geometry is Euclidean, because the coordinate transformation from physical to virtual space does not introduce intrinsic curvature [25]. In contrast, in our case (figure 1), the virtual space is curved: electromagnetic waves propagating in a plane with the refractive-index profile of Maxwell's fish eye behave as if they were confined to the surface of a virtual sphere [31], a curved space with non-Euclidean geometry [32].

To understand why Maxwell's fish eye can make perfect images, imagine light confined to the curved geometry of the sphere [33] (figure 1). Any source can be regarded as a collection

of point sources, so it suffices to investigate the wave produced by a single point source of arbitrary position on the sphere. A wave propagates from the point of emission round the sphere and focuses at the antipodal point; this corresponds to emission from a point in the plane of the actual device and focusing at another point. The wave propagating round the virtual sphere would come to the image point and then continue to travel back to the source. At the image it only turns into an exact inward-going wave if it is extracted at the image point [34, 35]. For this, one could employ an active drain synchronized with the time of arrival at the image, as in the demonstration of subwavelength imaging using far-field time reversal [35], but our experiments show that a completely passive outlet has the same effect: the outlet naturally extracts the electromagnetic wave as if it were a source run in reverse; a point source thus appears as a point image. Of course, the outlet must be at the correct image point, which is natural in imaging: for example, in a charged-coupled device (CCD) array only the detector at the correct point should fire. An array of outlets plays the role of a detector array or of the photosensitive molecules in a photographic substance. Our experiments show that, given a choice of outlets, i.e. a choice of detectors, the wave naturally focuses at the correct image positions[6].

Note that Maxwell's fish eye is an unusual 'lens' where both the source and the image are inside it, but in other proposals for perfect imaging with positive refraction [37], the source and the image can be in empty space (and in three dimensions (3D)). It may also be possible to make magnifying perfect lenses [38]. Essential for perfect imaging seems to be the feature that all rays from the source focus at the image, which is possible in a curved optical geometry [32], whereas in ordinary lenses only forward-propagating waves are imaged.

We have implemented Maxwell's fish eye for microwave radiation confined between two parallel metal plates constituting a planar waveguide [39]. Our device (figure 2) is inserted between the plates; its profile of refractive index n lets microwaves in the plane behave as if they were propagating on the surface of a half-sphere. The device is surrounded by a metal mirror such that the waves together with their mirror image correspond to waves on the complete virtual sphere (figure 1) of Maxwell's fish eye [9]. Our device is made of concentric layers of copper circuit board with etched-out structures that shape its electromagnetic properties (together with additional filling material). It resembles a microwave cloaking device [40] or a transmuted Eaton lens [41] (except that the fish-eye structures respond to the electric and not the magnetic field). Our structures are designed [41, 42] for non-resonant operation such that the device can perform perfect imaging over a broad band of the spectrum. The device has a radius of 5 cm, a thickness of 5 mm and fits exactly between the metal plates of the waveguide. The plate separation is chosen such that only microwaves with an electric field perpendicular to the plates can travel inside, because only for electromagnetic waves of this polarization does a material with electric permittivity $\varepsilon = n^2$ appear to curve space perfectly [9, 25].

As sources, we employ coaxial cables inserted through the bottom plate. The cables have an outer diameter of 2.1 mm, 1.68 mm teflon isolator and 0.5 mm inner conductor; the latter is exposed by 4.5 mm in the device for creating an approximate line source. Through the source cables, we inject microwave radiation of free-space wavelength $\lambda_0 = 3$ cm generated by a vector network analyzer (HP 8722D) that doubles as a synthesizer and an analyzer. The

---

[6] In the Feynman lectures [36], when discussing outward- and inward-going spherical waves, the reader is reminded that Maxwell's equations are time reversible. Consequently, an electromagnetic wave can be as perfectly focused at a point as it can be created by a point source [34], provided that the wave is time reversed and then detected at the image by a time-reversed source, a drain. We show here that both the effect of the time reversal and the field localization can be achieved with completely passive materials and without prior knowledge of the field.
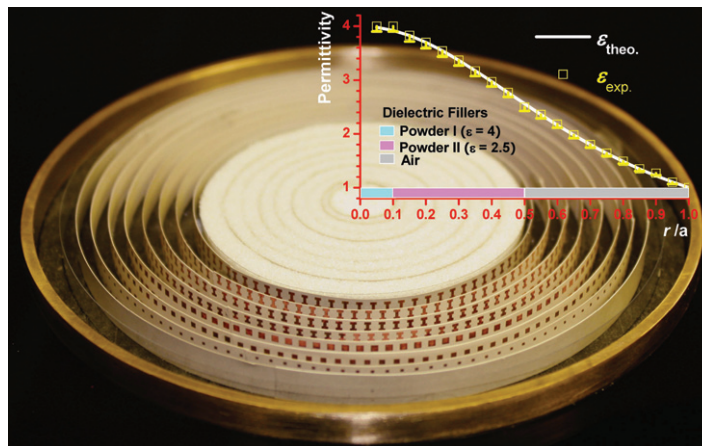
Figure 2. The device. Copper structures on concentric layers of circuit board and dielectric fillers surrounded by a circular metal mirror create the geometry of the sphere (figure 1) for microwave radiation with the electric field pointing in the vertical direction. The diagram shows the designed profile of the electric permittivity $\varepsilon = n^2$ at each layer of the device compared with Maxwell's theoretical formula (A.1).

outlets are coaxial cables as well, inserted through the top and/or the bottom plate. They lead back to the vector network analyzer for detection or terminate in impedance-matched absorbers, depending on their role in our experiments. They act as passive outlets and do not cause significant reflections. We vary the exposure lengths of the inner conductors in order to vary the electromagnetic cross sections of the cables. There we trade off efficiency for resolution. An outlet with 4.5 mm exposure is perfectly matched to the source and therefore has maximal extraction efficiency [43], but also a cross section of about half the wavelength [44], which is not suitable for subwavelength detection. Outlets with 2 mm exposure are optimal for resolving subwavelength features of the field, because their cross section is comparable to the structure size in our device, but their efficiency is lower. An outlet with no exposure does not localize the wave, because its cross section is too small, but merely scans the local field with minimal distortion. The bottom plate of the waveguide is movable laterally relative to the top plate with 1 mm step size [39]. In order to scan the field, we insert an outlet with no exposure through the top and measure the signal while moving the bottom plate.

Figure 3(a) illustrates the schemes of two experiments for probing the behavior of Maxwell's fish eye and comparing it with theory [9, 13, 21]. In the first experiment, we scan the field produced by a source without an outlet at the image. In the second experiment, we place an outlet optimized for power extraction at the image point. Without outlet (figure 3(b)), the field forms a standing wave where the radiation arriving at the image is reflected back to the source. No subwavelength focus is formed; the subwavelength features near the image originate from the structure of the material used to implement Maxwell's fish eye, the rings of the circuit board (figure 2). As the wave attempts to focus with perfect precision before being reflected back, the subwavelength structure of the device near the image becomes apparent. The potential of perfect imaging is already there, but it is only realized if the wave is given an outlet at the image (figure 3(c)). In this case, we obtain a running wave that develops a subwavelength spike. Both cases are in excellent agreement with theory (see the appendix).
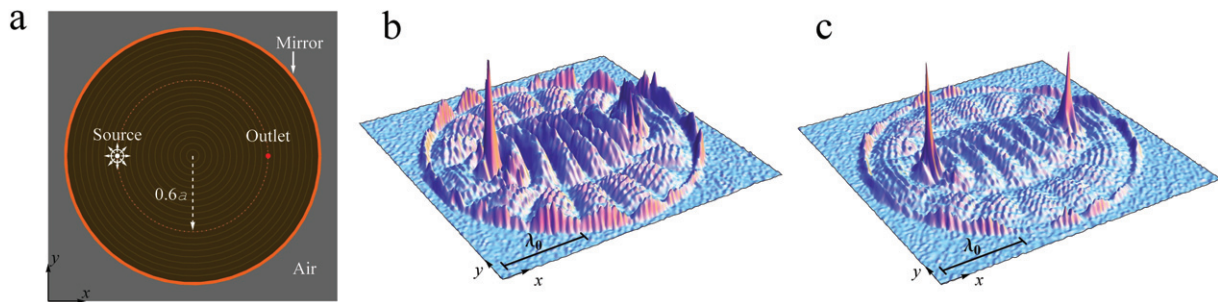
Figure 3. Field pattern. (a) Scheme of two imaging experiments of a point source without the outlet (b) and with the outlet (c) at the image point; λ_0 indicates the free-space wavelength of 3 cm. The field intensity is scanned. Without the outlet, no subwavelength focus is formed, whereas with the outlet, a sharp spike appears at the image.

The acid test for imaging is the resolution between two point sources. In a third experiment, we thus insert two source cables with 0.2λ distance from each other where λ denotes the local wavelength λ_0/n. In ordinary imaging [1], the two sources would not be resolvable. We capture the image with an array of ten outlets of 2 mm exposure that are inserted in the bottom plate in an arc with 0.05λ spacing between them; they represent a detector array. Two of the outlets are at the correct image points, but the others are not; for perfect imaging, only the detectors at the correct points should fire. We do not directly monitor the field intensity extracted by the outlets; their cables terminate in absorbers, because it is experimentally easier to scan the field localized at the outlets. As the intensity at the outlets is proportional to the extracted field intensity, this procedure gives the intensity profile recorded by a detector array. For scanning the field at the image, we insert another outlet of the same type (2 mm exposure) through the top plate (for scanning the field at the source we use outlets with no exposure). The scanning outlet is connected to the vector network analyzer for measuring the throughput. We move the top outlet in discrete steps along the arc and record the intensity. Figure 4 shows that the field localizes on its own near the outlets at the correct image positions. The localization is not an artifact of the outlets, in contrast to what was claimed in the controversy about perfect imaging with positive refraction [12], [14]–[16], [19, 20], because otherwise all outlets within a spot of $\lambda/2$ would enhance the field intensity. The two subwavelength sources are clearly resolved in the image, which unambiguously proves subwavelength imaging with positive refraction.

We have thus proved by experiment that the imaging resolution in Maxwell's fish eye is no longer limited by the wave nature of electromagnetic radiation, but rather by the structure of the material[7], which in our case is approximately 0.1λ. With unstructured materials—not metamaterials—such as graded-index materials or tapered waveguides [23, 45], the imaging resolution can in principle be made perfect.

Acknowledgments

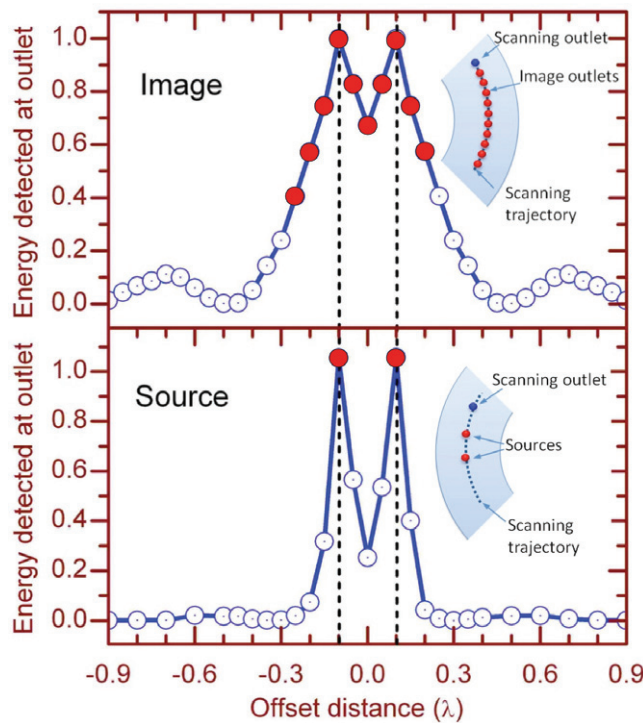[7] We used a structured metamaterial because it was cheap to make.

Figure 4. Imaging. Source: two sources (red dots) are placed 0.2λ apart where λ is the local wavelength; their scanned field is shown. Image: an array of ten outlets (red dots) are arranged in an arc in the bottom plate; they act like a detector array. A single outlet (blue dot) inserted through the top plate is moved along the arc over the image outlets and records the intensity. The picture shows the measured intensity normalized with respect to the maximal intensity. The red dots indicate the positions where outlets are present. This detector array clearly resolves the two sources, which proves subwavelength imaging.

Appendix. Theory and experiment

In this appendix, we compare theory with experiment. Let us briefly summarize the theory [9, 13, 21]. For simplicity, we describe the Cartesian coordinates x and y in the plane of the waveguide in units of the device radius a. It is convenient to combine the two coordinates in one complex number $z = x + iy$. In this notation and with our units, the refractive-index profile of Maxwell's fish eye reads [8, 9]

$$n = \frac{2}{1 + |z|^2}. \tag{A.1}$$

Consider stationary electromagnetic waves with wavenumber k (in our units) and electric field polarized in the vertical direction. In this case, the electric field strength is characterized by only one scalar complex Fourier amplitude E that varies in the z-plane; we denote it by $E(z)$. We assume that the wave propagates inside a material with electric permittivity $\varepsilon = n^2$ and index profile (A.1) surrounded by a perfect mirror at $r = 1$. Theory [13, 21] shows that the field of a
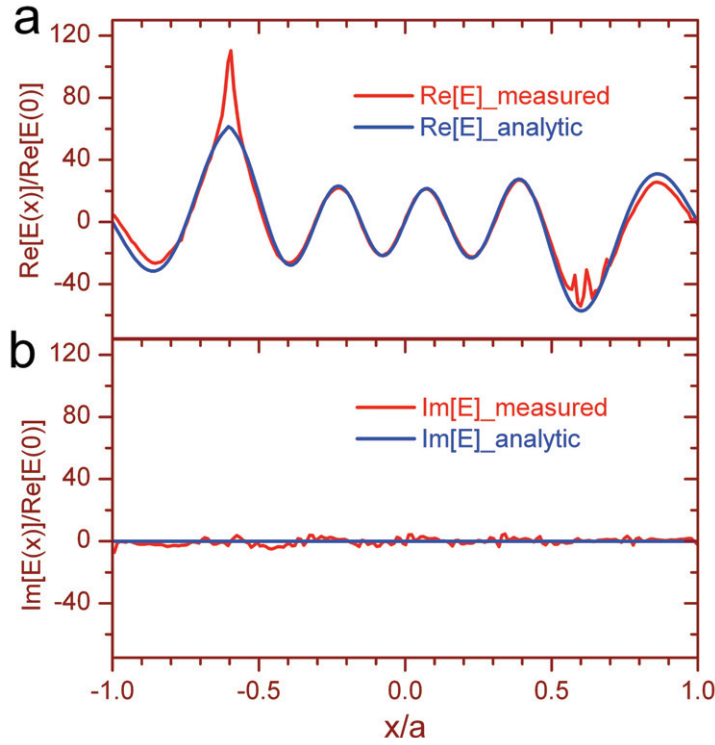
Figure A1. Comparison with theory for radiation without outlet. The field amplitude scanned along the line between the source and the outlet is compared with the analytical formula (A.2). The figure shows a standing wave in very good agreement with theory; the subwavelength features near the image originate from the structures of the material used to implement the fish eye mirror; the deviation near the source is due to its imperfection.

perfect line source without outlet at the image is given by the exact expressions

$$E(z) = G(z) - G(1/z^*), \quad G = \frac{P_\nu(\zeta)}{4\sin(\nu\pi)}, \tag{A.2}$$

where P_ν are Legendre functions [46] with the index

$$\nu = \frac{1}{2}\left(\sqrt{4k^2+1}-1\right). \tag{A.3}$$

For the variable ζ of the Legendre functions, we have [9]

$$\zeta = \frac{|z'|^2-1}{|z'|^2+1}, \quad z' = \frac{z-z_0}{z_0^* z + 1}, \tag{A.4}$$

where z_0 denotes the coordinates x_0 and y_0 of the line source in complex representation $z_0 = x_0 + iy_0$. The wave function (A.2) develops a logarithmic singularity at the source point that appears as the sharp peak in the measured intensity (figure 3(b)). The electromagnetic field forms a standing wave [13] with real wave function (A.2), where the radiation bounces back and forth in the device. In our experiments, we are able to measure both the real and the imaginary part of the oscillating electromagnetic wave—they correspond to the in-phase and out-of-phase components of the scanned field. For this, the scanning cable is fed into the
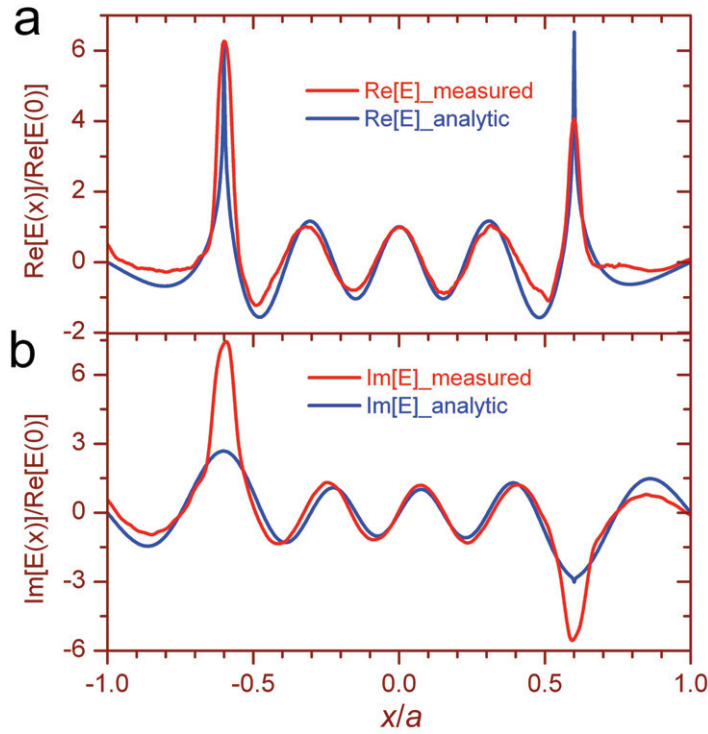
Figure A2. Comparison with theory for the wave with the outlet. The field amplitude scanned along the line between the source and the outlet is compared with the analytical formula (A.5). The figure shows a running wave with complex wave function in good agreement with theory; the sharp spike of Re(E) is a nearly perfect image of the source.

vector network analyzer where the signal is measured and decomposed into in-phase and out-of-phase components with respect to the synthesized field. Figure A.1 compares the results of our measurements with our analytical formulae: theory and experiment agree very well, except near the source where its finite cross section becomes apparent; we do not have an ideal line source. Our measurements confirm that without outlet, the wave is real and so a standing wave is formed, which cannot create a perfect image [13]. One sees that instead of a sharp spike, a diffraction-limited spot appears.

All it takes to form a sharp image is an outlet for the radiation. An ideal point detector plays the role of such an outlet, absorbing radiation at the image point but not elsewhere. This detector will only fire when it is placed at the correct position. In this case, we obtain a running wave with the wave function [9]

$$E(z) = G(z) - G(1/z^*), \quad G = \frac{P_\nu(\zeta) - e^{i\nu\pi} P_\nu(-\zeta)}{4\sin(\nu\pi)} \tag{A.5}$$

and expressions (A.3) and (A.4). The wave function (A.5) develops two logarithmic singularities [9] within the region $|z| < 1$ of the device, one at the source z_0 and one at the image point

$$z_0' = -z_0. \tag{A.6}$$

This means that the wave forms an exact image with a resolution not limited by the wave nature of light. The singularity at the image turns out [9] to carry the phase factor $\exp(i\pi\nu)$, so the

phase delay is $\pi\nu$. Figure A.2 shows that formula (A.5) agrees well with our data, apart from imperfections due to the finite electromagnetic cross section of the source and the image. The deviations are particularly strong in the imaginary part of the Fourier amplitude for reasons we do not fully understand yet. One sees that the field forms a running wave with a complex wave function. The wave disappears through the outlet at the focal point in a perfect image. Only the detected field is imaged with point-like precision, but detection is the very point of imaging.

References

[1] Abbe E 1873 *Arch. Mikrosk. Anat.* **9** 413
[2] Pendry J B 2000 *Phys. Rev. Lett.* **85** 3966
[3] Stockman M I 2007 *Phys. Rev. Lett.* **98** 177404
[4] Fang N, Lee H, Sun C and Zhang X 2005 *Science* **308** 534
[5] Jacob Z, Alekseyev L V and Narimanov E 2006 *Opt. Express* **14** 8247
[6] Liu Z, Lee H, Xiong Y, Sun C and Zhang X 2007 *Science* **315** 1686
[7] Lerosey G, de Rosny J, Tourin A and Fink M 2007 *Science* **315** 1120
[8] Maxwell J C 1854 *Camb. Dublin Math. J.* **8** 188
[9] Leonhardt U 2009 *New J. Phys.* **11** 093040
[10] Leonhardt U and Philbin T G 2010 *Phys. Rev.* A **81** 011804
[11] Benitez P, Miñano J C and González J C 2010 *Opt. Express* **18** 7650
[12] Blaikie R J 2010 *New J. Phys.* **12** 058001
[13] Leonhardt U 2010 *New J. Phys.* **12** 058002
[14] Guenneau S, Diatta A and McPhedran R C 2010 *J. Mod. Opt.* **57** 511
[15] Sun F and He S 2010 *Prog. Electromagn. Res.* **108** 307
[16] Merlin R 2010 *Phys. Rev.* A **82** 057801
[17] Leonhardt U and Philbin T G 2010 *Phys. Rev.* A **82** 057802
[18] Leonhardt U and Sahebdivan S 2011 *J. Opt.* **13** 024016
[19] Merlin R 2011 *J. Opt.* **13** 024017
[20] Kinsler P and Favaro A 2011 *New J. Phys.* **13** 028001
[21] Leonhardt U 2011 *New J. Phys.* **13** 028002
[22] González J C, Benitez P and Miñano J C 2011 *New J. Phys.* **13** 023038
[23] Smolyaninova V N, Smolyaninov I I, Kildishev A V and Shalaev V M 2010 *Opt. Lett.* **35** 3396
[24] Gabrielli L H, Leonhardt U and Lipson M 2010 arXiv:1007.2564
[25] Leonhardt U and Philbin T G 2010 *Geometry and Light: The Science of Invisibility* (New York: Dover)
[26] Leonhardt U 2006 *Science* **312** 1777
[27] Pendry J B, Schurig D and Smith D R 2006 *Science* **312** 1780
[28] Shalaev V M 2008 *Science* **322** 384
[29] Chen H, Chan C T and Sheng P 2010 *Nat. Mater.* **9** 387
[30] Leonhardt U and Philbin T G 2006 *New J. Phys.* **8** 247
[31] Luneburg R K 1964 *Mathematical Theory of Optics* (Berkeley, CA: University of California Press)
[32] Leonhardt U and Tyc T 2009 *Science* **323** 110
[33] Schultheiss V H, Batz S, Szameit A, Dreisow F, Nolte S, Tünnermann A, Longhi S and Peschel U 2010 *Phys. Rev. Lett.* **105** 143901
[34] Quabis S, Dorn R, Eberler M, Glöckl O and Leuchs G 2000 *Opt. Commun.* **179** 1
[35] de Rosny L and Fink M 2002 *Phys. Rev. Lett.* **89** 124301
[36] Feynman R P, Leighton R P and Sands M 2006 *The Feynman Lectures on Physics* vol 2 (San Francisco, CA: Addison-Wesley)
[37] Miñano J C 2006 *Opt. Express* **14** 9627
[38] Tyc T and Sarbort M 2010 arXiv:1010.3178

[39] Zhao L, Chen X and Ong C K 2008 *Rev. Sci. Instrum.* **79** 124701

[40] Schurig D, Mock J J, Justice B J, Cummer S A, Pendry J B, Starr A F and Smith D R 2006 *Science* **314** 977

[41] Ma Y G, Ong C K, Tyc T and Leonhardt U 2009 *Nat. Mater.* **8** 639

[42] Smith D R and Pendry J B 2006 *J. Opt. Soc. Am.* B **23** 391

[43] Marques R, Freire M J and Baena J D 2006 *Appl. Phys. Lett.* **89** 211113

[44] Cornbleet S 1976 *Microwave Optics: The Optics of Microwave Antenna Design* (London: Academic)

[45] Miñano J C, Benitez P and González J C 2010 *New J. Phys.* **12** 123023

[46] Erdélyi A, Magnus W, Oberhettinger F and Tricomi F G 1981 *Higher Transcendental Functions* vol 1 (New York: McGraw-Hill)